MultiCraft

International Journal of Engineering, Science and Technology
Vol. 3, No. 4, 2011, pp. 284-296

INTERNATIONAL JOURNAL OF ENGINEERING, SCIENCE AND TECHNOLOGY

www.ijest-ng.com

Correlation between pipe bend geometry and allowable pressure in pipe bends using artificial neural network

A.R. Veerappan[*] and S. Shanmugam

Department of Mechanical Engineering, National Institute of Technology Tiruchirappalli, INDIA
[*]Corresponding Author: e-mail: aveer@nitt.edu, Tel +91-431-2503416, Fax +91-431-2500133

Abstract

Determination of allowable pressure, which is one of the important criteria to evaluate the acceptability of pipe bends with shape irregularities, is complex as the analytical solution of the problem involves solution of complex differential equations. Artificial Neural Network (ANN) is used in this paper to determine the allowable pressure ratio for pipe bends with varied range of ovality and thinning/thickening, pipe ratio and bend ratio. A set of numerical data of pipe bends with shape irregularities obtained from ANSYS analysis is used in ANN to obtain a mathematical relationship between various design parameters of pipe bends namely pipe diameter, wall thickness, bend radius, ovality, thinning/thickening and the internal pressure load. The ANN result is in close agreement with the numerical output obtained from ANSYS.

Keywords: Pipe bends, Pipe ratio, Bend ratio, Ovality, Thinning, Optimum finite element mesh, Artificial neural network

1. Introduction

Pipe bends are used extensively in power plants to convey fluids and to change the direction of the fluids flowing inside the pipes. Bending of pipes with circular cross section is of considerable importance in the manufacture of boilers and the construction of pipe lines. Although the selection of a pipe bend manufacturing process for a specific case is influenced by several factors the most frequent methods of bending of pipes are bending with a mandrel and without a mandrel. During forming process of pipe bends, the outer fibre of the pipe bends thin down, which leads to a phenomenon known as thinning. The pipe bends also become oval due to manufacturing process (Patel et al, 2004). The pipe bends with ovality and thinning (shape irregularities) are subject to higher stresses. The ovality and thinning beyond a certain level will impair the safe operation of the pipe bends and the components to which they are attached. The present practice of accepting or rejecting pipe bends is based on the induced levels of ovality and thinning. Hence knowledge of the stresses induced under various loading conditions for varying ovality and thinning is required to determine the acceptability of pipe bends. But many analyses in pipe bends rely on the assumptions of constant wall thickness along the contour of the pipe's cross section and no initial ovality (Cherniy, 2001, Hyde et al., 2002, Cherniy, 2003, Hyde et al., 2002, Hyde et al., 2005). Hence, an attempt is made in this paper to determine the allowable pressure in pipe bends with ovality and thinning subjected to internal fluid pressure. A relationship between the allowable pressure and ovality, thinning, pipe ratio and bend ratio was established using ANN. The data obtained from FEM was used to train the ANN in order to establish the relationship. The results of allowable pressure obtained from the equation were found to be in good agreement with that obtained from ASME codes.

2. Generation of Input Data to ANN

2.1. Assumptions made: The material of the pipe bend is assumed to be homogeneous isotropic. Linear elastic behaviour of the material is considered. The loading of the pipe bend is considered under steady state. Only static stress analysis is carried out. The pipe bend is also assumed to become a perfect ellipse after bending. The thinning is considered to be equivalent to the thickening. The major axis of the elliptical shape of pipe bend is assumed to be perpendicular to the plane of bending of pipe bend. The minor

axis of the elliptical shape of pipe bend is assumed to be in the plane of pipe bend. The pipe bend is assumed to be smooth, without ripples and flattening.

*2.2. Definitions of shape irregularities:*The following definitions [Nayyar, 2000, LI Xue-tong et al, 2006, Jochen Weber et al, 2005] in brief are presented in brief with reference to the Fig. 1. They are all self explanatory.

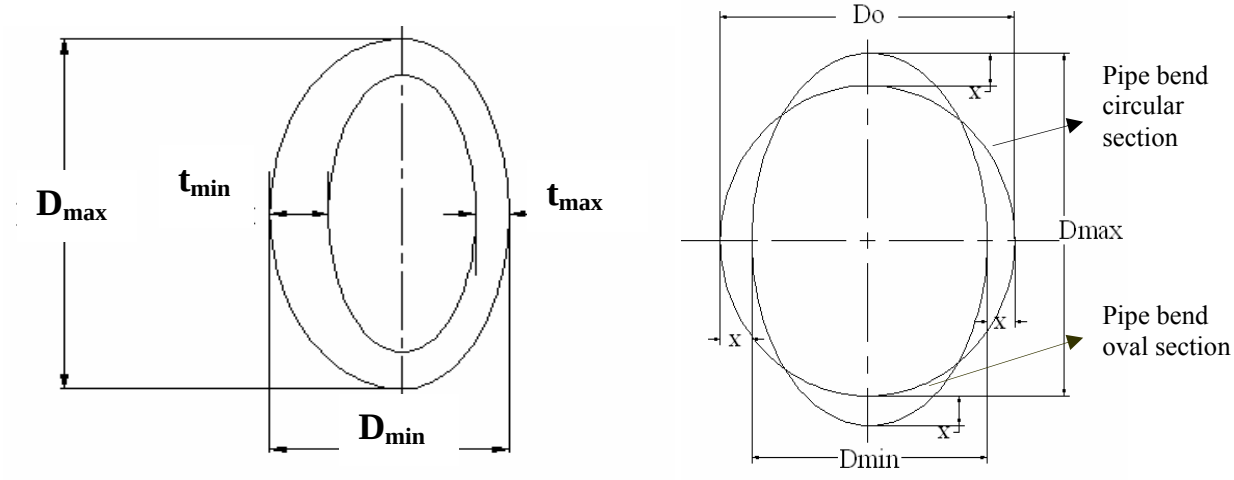

Figure 1. Pipe bend cross section with shape irregularities

1. Per cent Ovality

$$C_O = \frac{D_{max} - D_{min}}{D_O} \times 100 \quad (1)$$

2. Per cent Thinning

$$C_t = \frac{t - t_{min}}{t} \times 100 \quad (2)$$

3. Per cent Thickening

$$C_{th} = \frac{t_{max} - t}{t} \times 100 \quad (3)$$

4. Maximum outer diameter

$$D_{max} = D_O + 2X \quad (4)$$

5. Minimum outer diameter

$$D_{min} = D_O - 2X \quad (5)$$

Substituting Eq.4 and Eq.5 in Eq.1 and then rearranging to obtain

$$X = \frac{C_O D_O}{400} \quad (6)$$

Since the per cent of thinning/thickening of the bend is known, the maximum and minimum thickness at the intrados and extrados respectively are calculated using Eq.2 and Eq.3

$$t_{min} = t - \frac{t \times C_t}{100} \quad (7)$$

$$t_{max} = t + \frac{t \times C_t}{100} \quad (8)$$

2.3. Determination of maximum stress intensity: The pipe bend section is created with the values of X, t_{max} and t_{min} using line and area commands. Both ends are closed with straight lines and since the section is symmetric only one half of it is modeled. The created areas are moved along x axis to a distance equal to bend radius R (Fig. 2 (a)). In order to generate the finite element mesh optimum number of elements in each of the models are found by trial and error method. The model is first meshed with auto generated PLANE 82 elements. Symmetric boundary constraints on the symmetric section are applied. Internal pressure load on the pipe bend inner surface is applied. Fig.2 (b) shows a typical finite element model with internal pressure load and boundary conditions. The model is solved for stress intensities after supplying the material properties. The nodes in the intrados, neutral and extrados sections are located and the stress values at these nodes are extracted.

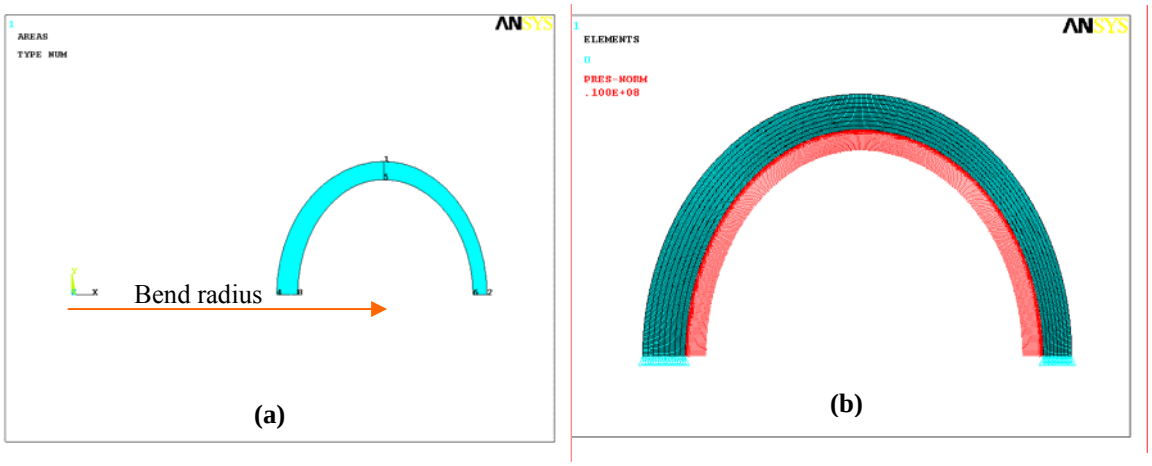

Figure 2: (a) Creation of model in ANSYS and (b) Optimum meshed model with constraints and load

The number of elements is then increased and the ANSYS (ANSYS inc., 2009) run is made. Fig. 3 shows the typical stress values at the three different sections of the model with the number of elements. It can be seen from the figure that the membrane and bending stresses decrease at the intrados and extrados and they converge when the number of elements is 3600 beyond which the stress has not decreased. The difference between successive stress intensity values has been kept at 10^{-3} MPa. The membrane stress at the neutral section also converges when the number of elements reaches 3600 while the bending stress at this section increases and converges when the number of elements is 1600. The three stress intensities have hence not changed beyond 3600 elements. The allowable pressure ratio at the intrados, neutral and extrados sections based on ASME code is calculated and the maximum allowable pressure ratio for the geometry is determined. The above procedure has to be repeated for getting data on the stress intensity at different sections on the model even if a change is introduced in any of the geometry parameters. Creation of models and computation of FEM results are definitely very cumbersome and time consuming whenever pipe bend geometry parameters are changed. With the application of ANN, the need for model creation and analysis for the desired set of inputs is eliminated. Besides, knowing the pipe bend geometry, the maximum allowable pressure can easily be determined.

2.4. Problem parameters: Pipe bends with specified shape and material properties are used (Table 1). The bend radii considered are 101.6 mm, 152.4 mm, 203.2 mm and 304.8 mm and tube thickness considered are 6.02 mm, 8.56 mm, 11.13 mm, and 13.49 mm (ASME, 2004). The values of thinning (and thickening) and the ovality considered are: 0%, 4%, 8%, 12%, 16% and 20%.

Table 1 Mechanical and chemical properties of the pipe bend

Pipe material	ASME SA234 WPB[ASME, 2008a]
Pipe internal pressure (P)	10 MPa (abs)
Pipe outside diameter (D_o)	114.3 mm
Pipe bend nominal thickness (T)	6.02 mm 8.56 mm 11.13 mm 13.49 mm
Pipe bend radius (R)	101.6 mm 152.4 mm 203.2 mm 304.8 mm
Bend angle(θ)	360° (Torus)
Pipe design temperature (t)	350°C
Elastic modulus (E)	178964 MPa
Poisson's ratio (Nu)	0.3
Stress analysis code	ASME section VIII, Division 2.

Chemical properties

COMPOSITION, %									
C	Mn	P	S	Si	Cr	Mo	Ni	Cu	V
0.3max	0.29-1.06	0.050 max	0.058 max	0.1 min	0.4 max	0.15 max	0.4 max	0.4 max	0.08 max

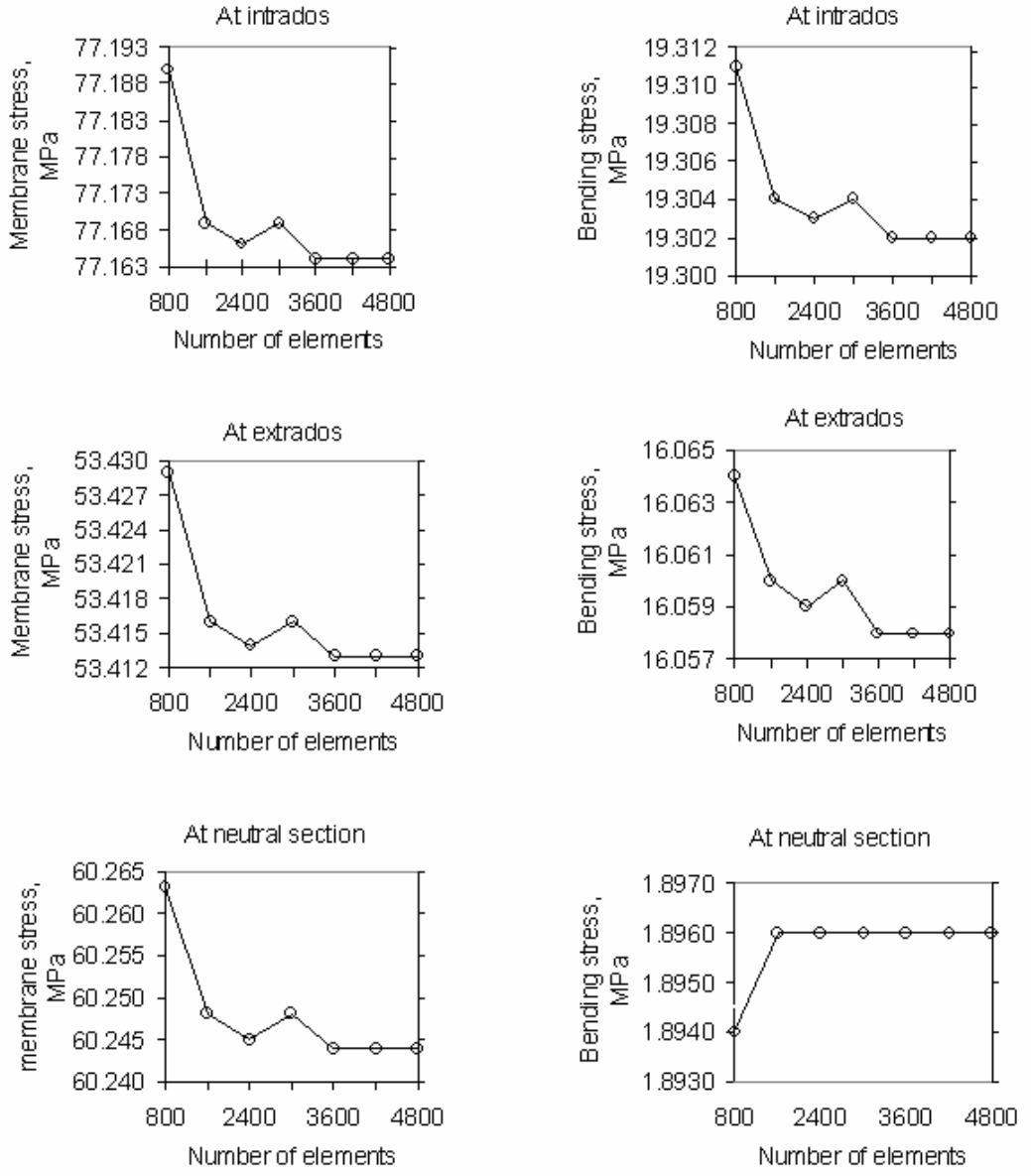

Figure 3. Finding optimum number of elements for generation of finite element mesh

2.5. Determination of allowable pressure ratio: The acceptability criteria used in the pressure vessels industry to evaluate the results of finite element stress analysis are as per ASME (ASME Section VIII, 2008, ASME Section I, 2008, ASME Power Piping, 2001)

$$P_m < k\,S_m \tag{9}$$

$$P_m + P_L < 1.5\,k\,S_m \tag{10}$$

$$P_m + P_L + P_b < 1.5\,k\,S_m \tag{11}$$

$$P_m + P_L + P_b + Q < 3S_{ch} = \frac{3(S_c + S_h)}{2} \quad (12)$$

$$P_m + P_L + P_b + Q + P_F < 2S_a \quad (13)$$

The local membrane stress P_L is absent in the case of pipe bends with internal pressure. Hence Eq. (10) is not applicable. As the stresses induced due to internal pressure in pipe bends is primary in nature, the stress Q is absent. Hence Eq. (12) is not applicable. As the pipe bend considered is subjected to 10000 fatigue load cycles, the allowable range of fatigue stress intensity is, as per ASME code, equal to twice the allowable stress (S_a) i.e., 2 x 275 = 550 MPa. This is not governing in the present stress analysis. Hence Eq. (13) is not governing. It is therefore required to consider Eq. (9) and Eq. (11) only in the present analysis.

Using the above acceptability criteria, the non-dimensional parameter - P/S_m are calculated as illustrated below.

Since k = 1 for normal loads, from Eq. (9),

$$P_m < S_m \quad (14)$$

Multiplying Eq. (14) by P and then rearranging it to obtain

$$\frac{P}{S_m} < \frac{P}{P_m} \quad (15)$$

Substituting $P_L = 0$ into Eq. (11),

$$P_m + P_b < 1.5S_m$$

$$S_m < \frac{(P_m + P_b)}{1.5}$$

$$\frac{P}{S_m} < \frac{1.5P}{(P_m + P_b)} \quad (16)$$

2.5.1. Sample calculation for computation of P/S_m

C_t=12% C_o=8% R = 101.2 mm t=6.02mm

1) At intrados

$$R_1 = \frac{P}{P_{im}} = \frac{10}{114} = 0.087$$

$$R_2 = \frac{1.5\,P}{(P_{im} + P_{ib})} = \frac{1.5 \times 10}{(114 + 19.41)} = 0.112$$

$$Ratio(R_i) = minimum(R_1, R_2) = 0.088$$

At neutral section

$$R_3 = \frac{P}{P_{nm}} = \frac{10}{79.91} = 0.125$$

$$Ratio(R_4) = \frac{1.5P}{(P_{nm} + P_{nb})} = \frac{1.5 \times 10}{(79.91 + 16.87)} = 0.155$$

$$Ratio(R_n) = minimum(R_3, R_4) = 0.125$$

At extrados

$$Ratio(R_5) = \frac{P}{P_{om}} = \frac{10}{82.26} = 0.122$$

$$Ratio(R_6) = \frac{1.5P}{(P_{om} + P_{ob})} = \frac{1.5 \times 10}{(82.26 + 5.813)} = 0.170$$

$$Ratio(R_o) = minimum(R_5, R_6) = 0.122$$

$$\frac{P}{S_m} = \frac{P}{P_m} = \frac{1.5P}{(P_m + P_b)} = minimum(R_i, R_n, R_o) = 0.088$$

The primary membrane, bending and peak stress values are obtained for all possible combinations of pipe bend geometry parameters. A typical value of these stresses are presented in Table 2. The table also shows the allowable pressure ratio calculated for each combination of ovality and thinning.

Table 2 A typical set of stresses at different sections and determination of P/S_m for R = 101.6 mm and t = 6.02 mm

C_t, %	C_o, %									
	0		4		8		12		20	
0	Pim = 140 Pib = 19.70	Pom = 74.29 Pob =13.95	Pim = 134 Pib = 19.45	Pom = 73.36 Pob =6.02	Pim = 128 Pib = 19.25	Pom = 72.37 Pob =4.26	Pim = 123 Pib = 19.15	Pom = 84.36 Pob =8.29	Pim = 121 Pib = 19.11	Pom = 108 Pob =14.16
	Pnm = 87.38 Pnb = 5.275	P/Sm = 0.072	Pnm = 83.50 Pnb = 5.734	P/Sm = 0.075	Pnm = 79.78 Pnb = 16.25	P/Sm = 0.078	Pnm = 76.23 Pnb = 26.33	P/Sm = 0.082	Pnm = 69.60 Pnb = 45.38	P/Sm = 0.083
4	Pim = 134 Pib = 19.70	Pom = 77.38 Pob =13.56	Pim = 129 Pib = 19.48	Pom = 76.41 Pob =5.45	Pim = 123 Pib = 19.31	Pom = 75.39 Pob =4.75	Pim = 118 Pib = 19.27	Pom = 87.85 Pob =8.84	Pim = 117 Pib = 19.27	Pom = 112 Pob =14.77
	Pnm = 87.43 Pnb = 5.023	P/Sm = 0.075	Pnm = 83.54 Pnb = 5.956	P/Sm = 0.078	Pnm = 79.83 Pnb = 16.44	P/Sm = 0.081	Pnm = 76.28 Pnb = 26.49	P/Sm = 0.085	Pnm = 69.66 Pnb = 45.46	P/Sm = 0.086
8	Pim = 129 Pib = 19.70	Pom = 80.75 Pob =13.14	Pim = 124 Pib = 19.51	Pom = 79.74 Pob =5.033	Pim = 119 Pib = 19.36	Pom = 78.68 Pob =5.261	Pim = 113 Pib = 19.36	Pom = 91.63 Pob =9.427	Pim = 112 Pib = 19.42	Pom = 117 Pob =15.415
	Pnm = 87.47 Pnb = 4.479	P/Sm = 0.077	Pnm = 83.58 Pnb = 6.202	P/Sm = 0.081	Pnm = 79.87 Pnb = 16.65	P/Sm = 0.084	Pnm = 76.32 Pnb = 26.66	P/Sm = 0.088	Pnm = 69.71 Pnb = 45.55	P/Sm = 0.086
12	Pim = 125 Pib = 19.69	Pom = 84.42 Pob =12.70	Pim = 119 Pib = 19.52	Pom = 83.37 Pob =4.831	Pim = 114 Pib = 19.41	Pom = 82.26 Pob =5.813	Pim = 109 Pib = 19.44	Pom = 95.75 Pob =10.05	Pim = 109 Pib = 19.54	Pom = 122 Pob =16.28
	Pnm = 87.51 Pnb = 4.448	P/Sm = 0.08	Pnm = 83.62 Pnb = 6.470	P/Sm = 0.084	Pnm = 79.91 Pnb = 16.87	P/Sm = 0.088	Pnm = 76.37 Pnb = 26.84	P/Sm = 0.09	Pnm = 69.76 Pnb = 45.64	P/Sm = 0.082
20	Pim = 116 Pib = 19.67	Pom = 92.87 Pob =11.72	Pim = 111 Pib = 19.54	Pom = 91.72 Pob =4.382	Pim = 107 Pib = 19.49	Pom = 90.51 Pob =7.048	Pim = 102 Pib = 19.57	Pom = 105 Pob =11.46	Pim = 102 Pib = 19.75	Pom = 134 Pob =18.54
	Pnm = 87.58 Pnb = 3.770	P/Sm =0.086	Pnm = 83.69 Pnb = 7.066	P/Sm = 0.09	Pnm = 79.98 Pnb = 17.36	P/Sm =0.094	Pnm = 76.44 Pnb = 27.22	P/Sm = 0.095	Pnm = 69.87 Pnb = 45.81	P/Sm = 0.075

3. Artificial Neural Networks

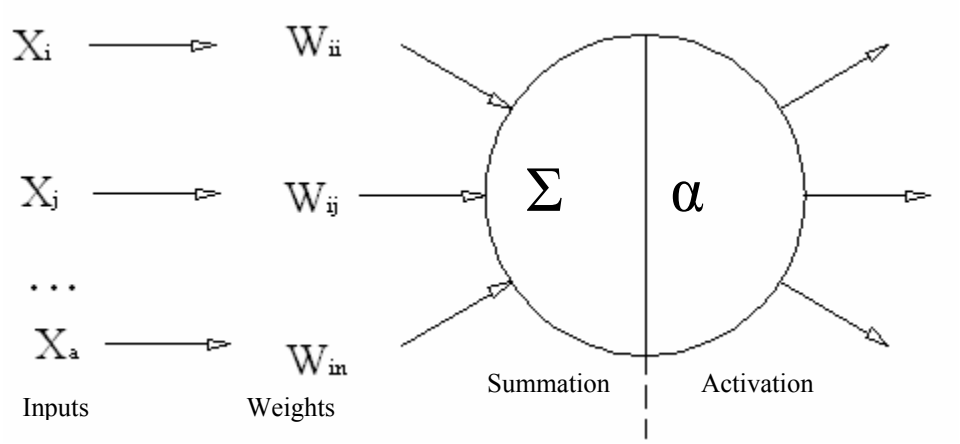

Figure 4. Information processing in artificial neural network

Artificial neural networks which are one of the most powerful computer modeling techniques are currently being used in many fields of engineering for modeling complex relationship **(**Ezugwu et al., 2005**).** Few published work is available in pipe bends using the technology of ANN. ANN has been used (Yu-Lin et al, 1996) to evaluate the failure bending moment full-scale pipes under internal pressure and external bending moment. The present study is on the application of ANN in modeling the relationship between the allowable pressure ratio and ovality, thinning, pipe ratio and bend ratio in pipe bends that are subject to various internal pressures.

The ANN modeling is carried out in two steps. The first step is to train the network whereas the second step is to test the network with data which were not used for training. As in nature, the network function is determined largely by the connections (weights) between elements. Fig. 4 shows how information is processed through a single node. The node receives weighted activation from other nodes through its coming connections. First these are added. The result is then passed through an activation functions, the outcome being the activation of the node. For each of the outgoing connections, this activation value is multiplied with the specific weight and transferred to the next node. A training set is a group of matched input and output patterns. This is used for the training of the network, usually by suitable adaptation of the synaptic weights. The outputs are the dependant variables that the network produces for the corresponding input. It is important that all the information that the network needs to learn is supplied to the network as a data set. When each pattern is read, the network uses the input data to produce an output, which is then compared to the desired output. If there is a difference, the connection weights are altered in such a direction that the error is decreased. After the network has run through all the input patterns, if the error is still greater than the maximum desired tolerance, the ANN runs through all the input patterns repeatedly until all the errors are within the required tolerance. When the training reaches a satisfactory level, the network holds the weights constant and the trained network can be used to take decisions, identify patterns, or define associations in new data sets not used to train it **(**Kalogirou, 1999, Kalogirou et al, 1999, Kalogirou, 2000, Kalogirou, 2001**).**

The P/S_m values obtained from ANSYS are used to train the ANN. The inputs to the network are thinning, ovality, R/D and D/T and the output is P/S_m. The back-propagation learning algorithm is used in a feed-forward, single hidden layer network. Tan-sigmoid transfer function is used as the activation function for both the hidden and output layers. Levenberg-Marquardt Back-propagation (Li Zhang & Ganesh Subbarayan, 2002, Christian Kanzow et al, 2005) training is repeatedly applied until satisfactory training is achieved. The Tan -sigmoid transfer function takes the form,

$$F(x) = \frac{e^{x} - e^{-x}}{e^{x} + e^{-x}} \tag{17}$$

where x is the weighted sum of the input. The log-sigmoid transfer function is given by

$$F(x) = \frac{1}{1 + e^{-x}}$$

The computer program is performed under MATLAB environment using the neural network toolbox. The data obtained from ANSYS for P/S_m are 576 of which 500 data are used for training purpose while the remaining are randomly selected and used as test data. The results showed good agreement thereby justifying the accuracy of the network. Fig. 5 shows the architecture of the ANN used for allowable pressure ratio prediction. The configuration 4-18-1 appears to be optimal for this application.

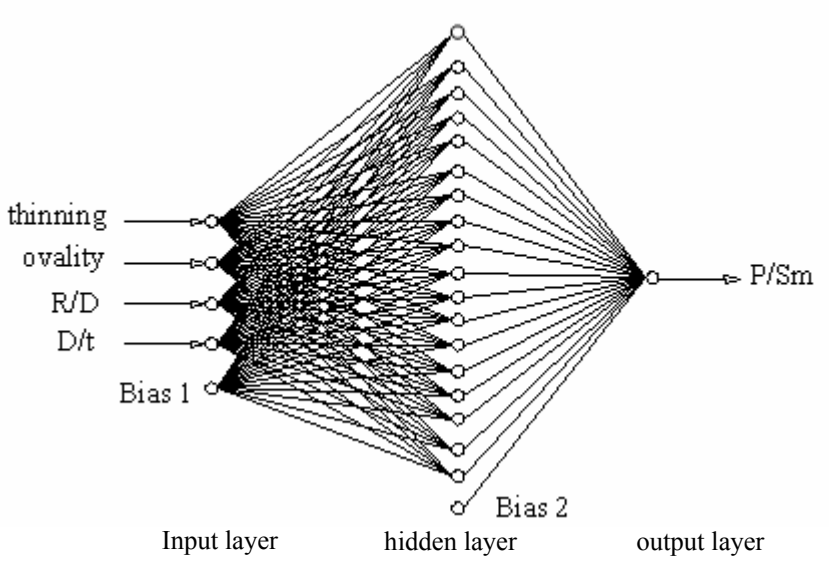

Figure 5. ANN model used for P/S_m

The network has been chosen in such a way that the maximum error is within 5% and the average error and standard deviation are within 1%. Network training is started with one hidden layer and four neurons and the neurons were increased until the desired level of tolerance as mentioned above was reached (Fig. 6).

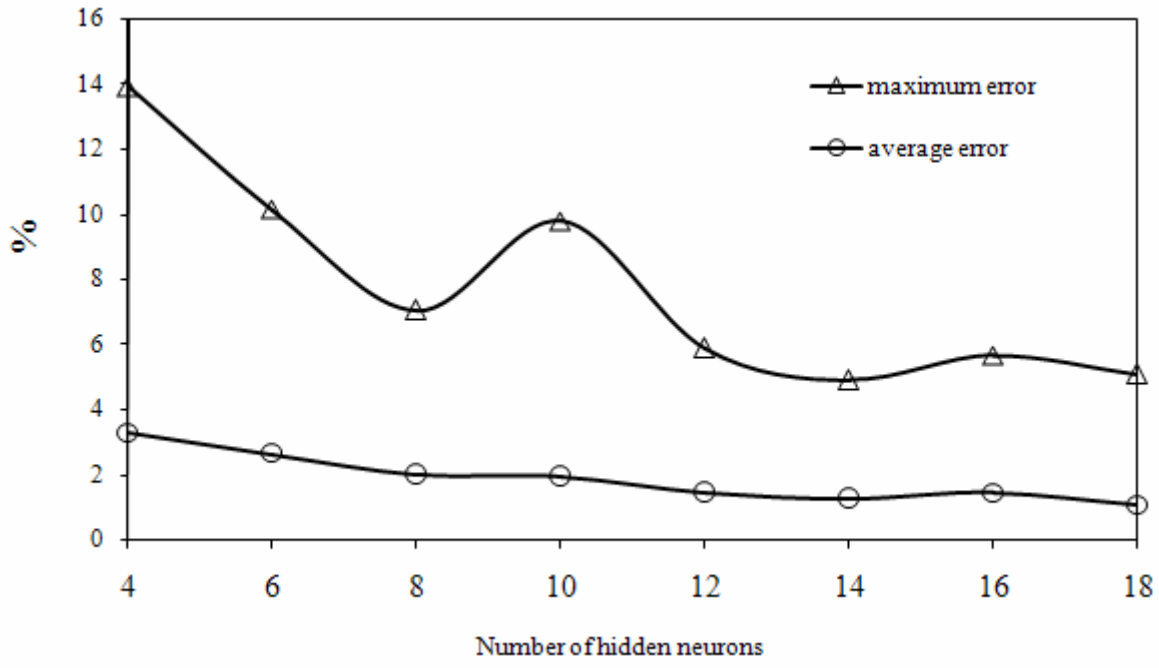

Figure 6. Maximum and average errors for tan sigmoid function

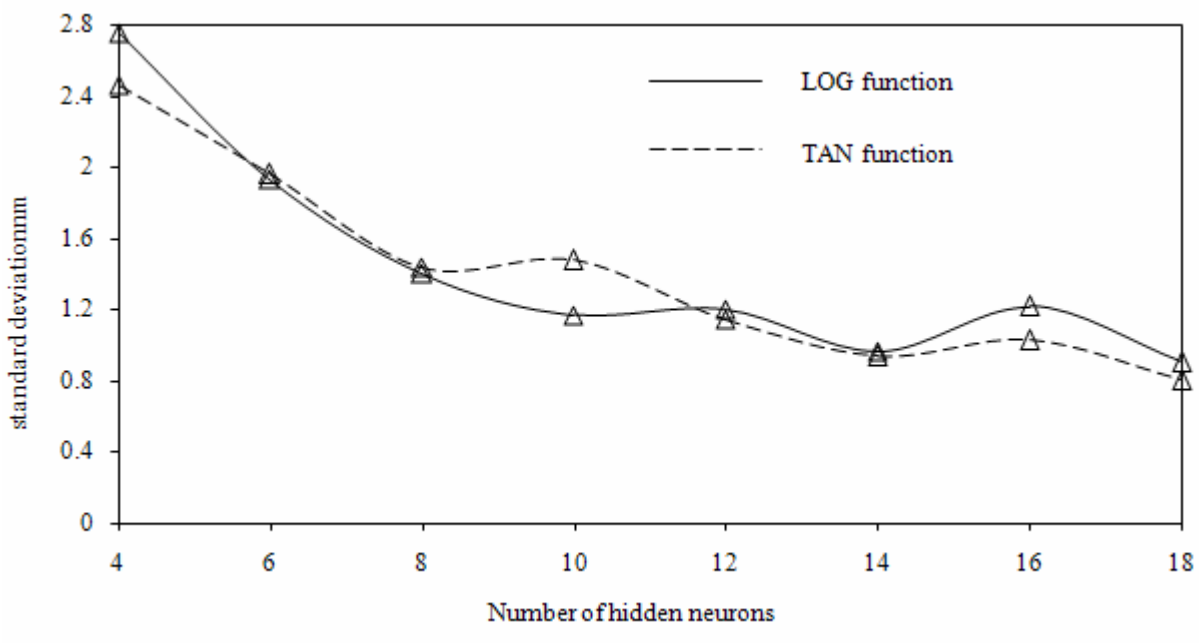

Figure 7. Comparison of standard deviation for log and tan sigmoid functions

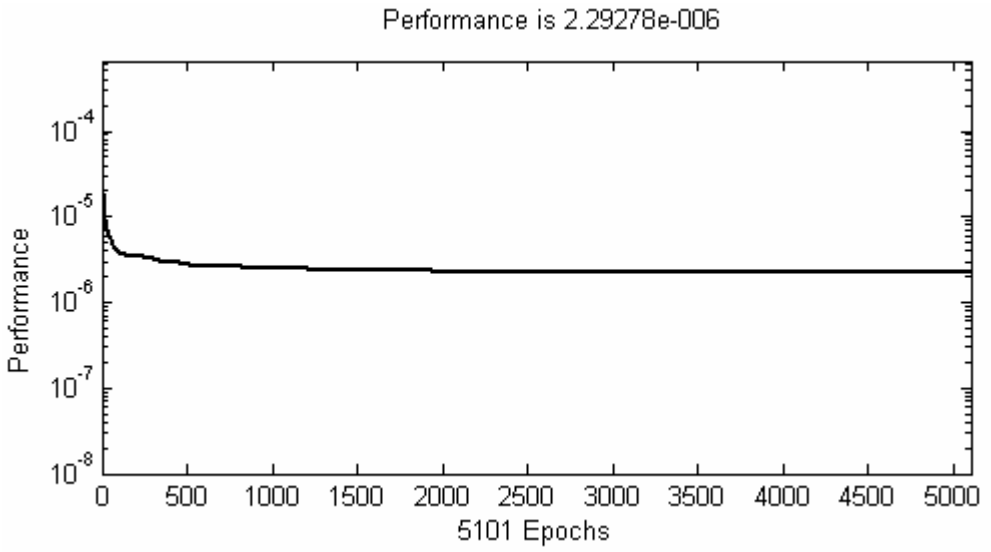

Figure 8. Training results based on 4-18-1 configuration

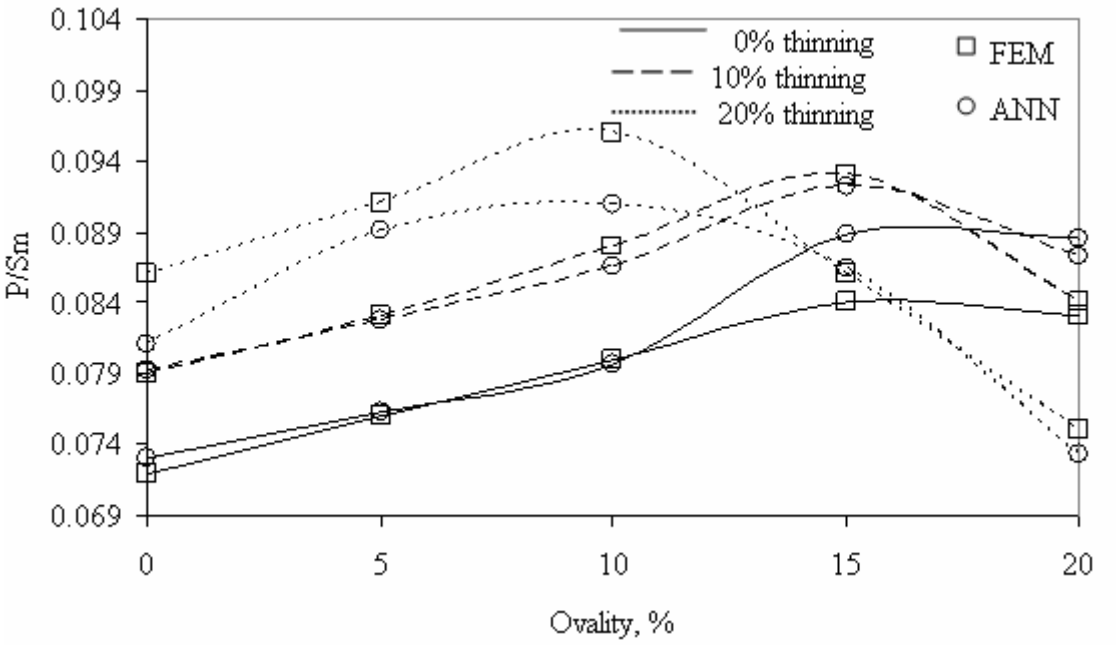

(a) Comparison between FEM and ANN for R/D = 0.89 and D/t = 18.98

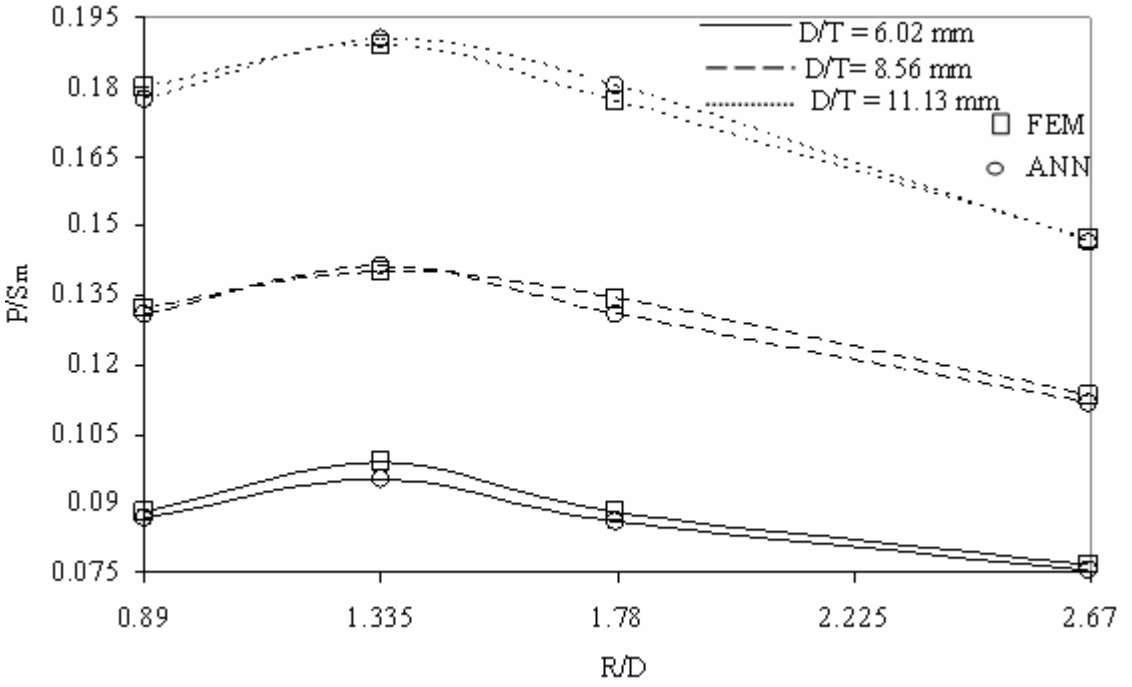

(b) Comparison between FEM and ANN for 10% ovality and 10% thinning

Figure 9, Comparison of ANN predicted values with the numerical output.

The Tan sigmoid and Log sigmoid non linear functions have been tried for their suitability as network functions for the data. The tan sigmoid function is used since it is found to have a lower standard deviation as shown in Fig. 7 while Fig.8 shows the decrease in the mean square error during the training process. The comparison of the output of ANN and FEM is presented in Fig. 9.

4. Results and discussion

To calculate the allowable pressure ratio (P/S_m), mathematical formulations have been derived from the resulting weights and activation functions used in ANN. As the coefficients obtained for both the training and testing of the ANN are extremely good, the results obtained can be assumed accurate. In the following formulas, terms A_1 to A_{18} represent summation function of each neuron of the hidden layer, These coefficients represent the weight values of the summation function of each neuron belonging to the hidden layer of the trained network. For this purpose, and for the case of P/S_m solution, eighteen equations are required as the neural network model has eighteen hidden neurons. In the output neuron, only one summation function is used, as only one output parameter exists which corresponds to allowable pressure ratio (P/S_m).

In order to calculate the P/S_m ratio the following equations are derived.

$$A_I = tanh\{a\,C_t + b\,C_o + c\,R/D - d\,D/T - e\} \quad (I = 1 \text{ to } 18) \tag{18}$$

I	a	b	C	d	e
1	0.0406	0.0764	1.8129	-0.0086	-3.5292
2	-0.0449	0.0622	0.1723	0.00266	0.1701
3	0.1627	-1.3513	-1.5155	-0.2094	8.0533
4	0.0595	0.0520	1.0619	-0.0217	-3.0445
5	0.0715	1.6361	2.3444	-0.0926	-34.4981
6	-0.3529	-7.1790	-31.7490	9.5206	49.2065
7	0.0162	-0.672	2.0355	-0.0912	1.1889
8	0.0439	-0.0613	-0.1833	-0.0206	-0.1838
9	0.0197	-0.1298	1.0166	0.0974	-2.8489
10	-0.0718	0.8366	-4.2414	1.1075	-18.1236
11	-0.1996	-0.0618	14.9192	2.2131	-43.6378
12	0.0768	0.0362	0.7679	-0.1528	1.6539
13	-0.0367	-0.0806	-0.6297	-0.0631	4.8964
14	-0.0194	0.1288	-1.0035	-0.0991	2.8491
15	-0.0542	-0.025	-0.8223	0.047	1.6191
16	-0.1105	0.1137	13.93	1.8259	-39.3669
17	-0.0025	-0.0258	-0.3211	0.2085	-0.273
18	0.0026	0.0229	0.3005	-0.2090	-0.3757

The expression to determine the allowable pressure ratio takes the following form

$$\frac{P}{S_m} = tanh(W + X + Y + Z) \tag{19}$$

Where

$$W = -0.04A_1 - 1.9446A_2 - 0.0052A_3 - 0.1090A_4 + 0.0077A_5$$

$$X = 0.0045A_6 + 0.0112A_7 - 2.0445A_8 - 0.9877A_9 - 0.0042A_{10}$$

$$Y = 0.0057A_{11} + 0.0276A_{12} + 0.0484A_{13} - 0.9877A_{14} - 0.1405A_{15}$$

$$Z = -0.0067A_{16} + 2.3758A_{17} + 2.4448A_{18} + 0.0255$$

5. Conclusions

The ANN is used to determine the allowable pressure ratio for pipe bends with shape irregularities subjected to internal pressure load. Equations have been derived from ANN, which eliminates the entire procedure of model creation and analysis in ANSYS to determine the allowable pressure ratio. In addition, known the pipe bend geometry, estimation of the allowable pressure can be done without prior knowledge of the concepts involved. This procedure can be extended to determine the allowable pressure for any set of inputs. Known the pipe bend geometry, calculation of allowable pressure will give an idea if the pipe will operate safely with the induced levels of ovality and thinning and hence the existing practice in industry to accept or reject pipe bends based on piping codes based on ovality and thinning can be improved. The present analysis can be extended to generate equations for a wide range of pipe and bend ratios to generalize the procedure further. For pipe bends, the acceptability results determined by neural network are in close agreement with the allowable pressure ratio calculated by the ASME code.

Nomenclature

C_o	:	per cent ovality
C_t	:	per cent thinning
C_{th}	:	per cent thickening
D_{max}	:	maximum outside diameter of pipe, mm
D_{min}	:	minimum outside diameter pipe, mm
D_o		nominal pipe diameter (mm)
E		Elastic modulus (MPa)
k		occasional load factor
P		allowable internal pressure for the pipe bend (MPa) (g)
P_b		average bending stress intensity across the thickness (MPa)
P_F		peak stress intensity (MPa)
P_L		local membrane stress intensity across the thickness (MPa)
P_m		average membrane stress intensity across the thickness (MPa)
Q		secondary stress intensity (MPa)
R		bend radius to neutral axis (mm)
S_a		allowable amplitude of stress intensity for "N" fatigue load cycles (MPa)
S_c		allowable stress intensity at ambient condition (MPa)
S_h		allowable stress intensity at deign temperature (MPa)
S_m		allowable stress intensity as per ASME Section VIII, Division 2, 2004 (MPa)
N		number of fatigue load cycles during the plant life (assumed to be 10,000)
T		pipe design temperature (° C)
t		nominal thickness of pipe (mm)
t_{max}		maximum pipe thickness (mm)
t_{min}		minimum pipe thickness (mm)
X		deviation from nominal pipe diameter due to irregular manufacturing process (mm)
Nu		Poisson's ratio
θ		pipe bend angle (degrees)
Suffix i		intrados section
Suffix n		neutral section
Suffix o		extrados section.

References

ASME, 2004. ASME Boiler and Pressure Vessel Code, SectionII: Materials Part A – Ferrous Material Specifications, p. 218.

ASME, 2008. Alternate Rules, ASME Boiler and Pressure Vessel Code - Section VIII, Division 2.

ASME, 2008, Power Boiler, ASME Boiler and Pressure Vessel Code - Section I.

ASME, 2008a, ASME Boiler and Pressure Vessel Code, Section II: Materials Part A- Ferrous Material Specifications, ASME, New York, p. 376.

ASME, 2001, Power Piping, ASME B31.1.

ANSYS 8.0 User Manual, 2003, Canonsburg, PA.

Cherniy. V.P. 2001. Effect of Curved Bar Properties on Bending of Curved Pipes. *Journal of Applied Mechanics*, Vol. 68, pp. 650 – 655.

Cherniy. V. P. 2003. The Bending of Curved Pipes With Variable Wall Thickness. *Journal of Applied Mechanics*, Vol. 70, pp. 253 – 259.

Christian Kanzow, Nobuo Yamashita and Masao Fukushima. 2005. Levenberg–Marquardt methods with strong local convergence properties for solving nonlinear equations with convex constraints. *Journal of Computational and Applied Mathematics*, Vol. 173, No. 2, pp. 321-343.

Ezugwu. E.O., Fadare. D.A., Bonney. J., Da Silva R.B. and Sales W.F. 2005. Modelling the correlation between cutting and process parameters in high-speed machining of Inconel 718 alloy using an artificial neural network. *International Journal of Machine Tools and Manufacture*, Vol. 45, pp. 1375-1385.

Hyde. T.H.,Sun. W. Williams J.A. 2002. Life estimation of pressurised pipe bends using steady-state creep reference rupture stresses. *International Journal of Pressure Vessels and Piping*, Vol. 79 pp. 799–805.

Hyde. T.H., Becker. A.A., Sun. W. Williams J.A. 2005. Influence of geometry change on creep failure life of 90° pressurised pipe bends with no initial ovality. *International Journal of Pressure Vessels and Piping*, Vol. 82, pp. 509–516.

Jochen Weber, Klenk A. and Rieke. M. 2005. A new method of strength calculation and lifetime prediction of pipe bends operating in the creep range. *International Journal of Pressure Vessels and Piping*, Vol. 82, pp. 77–84.

Kalogirou. S.A. 1999. Applications of artificial neural networks in energy systems. A review. *Energy Conversion and Management*, Vol. 40, pp. 1073-1087.

Kalogirou. S.A. Panteliou S. and Dentsoras. A. 1999. Modeling of Solar Domestic Water Heating Systems Using Artificial Neural Networks. *Solar Energy*, Vol. 65, pp. 335-342.

Kalogirou S.A. and Bojicb M. 2000. Artificial neural networks for the prediction of the energy consumption of a passive solar building. Energy, Vol. 25, pp. 479-491.

Kalogirou. S.A. 2001. Artificial neural networks in renewable energy systems applications: a review. *Renewable and Sustainable Energy Reviews*, Vol. 5, pp. 373-401.

LI Xue-tong, WANG Min-ting, DU Feng-shan. and XU Zhi-qiang. 2006. FEM Simulation of Large Diameter Pipe Bending Using Local Heating. *Journal of Iron and Steel Research, International*, Vol. 13, No. 5, pp. 25-29.

Li Zhang and Ganesh Subbarayan. 2002. An evaluation of back-propagation neural networks for the optimal design of structural systems: Part II.Numerical evaluation. *Computer Methods in Applied Mechanics and Engineering*, Vol. 191, pp. 2887–2904.

Nayyar. M. L. 2000. Piping handbook, 7th Ed. McGraw-Hill, A269.

Patel. B. P., Munot. C. S., Gupta. S. S., Sambandam C.T. and Gunapathi. M. 2004. Application of Higher Order Finite Element for Elastic Stability Analysis of Laminated Cross-Ply Oval Cylindrical Shells. *Finite Elem. Anal. Design*, Vol. 40, pp. 1083–1104.

Yu-Lin, Shi-Ming and Shu-Ho Dai. 1996. Artificial neural network technology as a method to evaluate the failure bending moment of a pipe with a circumferential crack. *International Journal of Pressure Vessels and Piping*, Vol. 68, pp. 1-6.

Biographical notes

AR. Veerappan received his M.E. from R.E.C., Tiruchirappalli in 1994 and Ph.D. from National Institute of Technology Tiruchirappalli in 2008. He received best thesis award for his research work. He is an Assistant Professor in the Department of Mechanical Engineering, National Institute of Technology Tiruchirappalli. His major research interests include Stress analysis in pressure vessels and Solar thermal. He is a member of Institution of Engineers (India).

Dr. S.Shanmugam is a Professor in the Department of Mechanical Engineering, National Institute of Technology Tiruchirappalli, India. He has more than 18 years of experience in teaching and research. His current area of research includes design of pressure vessel and piping, Stress analysis of machine elements, solar energy applications, heat transfer, Energy and sustainable development and simulation methods.

Received March 2011
Accepted July 2011
Final acceptance in revised form July 2011